ELSEVIER

Coordination Chemistry Reviews 226 (2002) 71–80

COORDINATION CHEMISTRY REVIEWS

www.elsevier.com/locate/ccr

Formation of superoxide–metal ion complexes and the electron transfer catalysis

Shunichi Fukuzumi [a,*], Hideki Ohtsu [a], Kei Ohkubo [a], Shinobu Itoh [b], Hiroshi Imahori [a]

[a] *Department of Material and Life Science, Graduate School of Engineering, Osaka University, CREST, Japan Science and Technology Corporation (JST), Suita, Osaka 565-0871, Japan*

[b] *Department of Chemistry, Graduate School of Science, Osaka City University, 3-3-138, Sugimoto, Sumiyoshi-ku, Osaka, 558-8585, Japan*

Received 11 April 2001; accepted 8 August 2001

Contents

Abstract

The formation of a variety of superoxide–metal complexes and their catalytic functions have been reviewed. The g_{zz}-values of the EPR spectra of superoxide–metal ion complexes vary significantly depending on the type of metal ions. From the deviation of the g_{zz}-value from the free spin value are determined the energy splitting values (ΔE) of π_g levels due to complex formation. The ΔE values correlate well with the catalytic reactivities of the metal ions in the electron transfer reduction of oxygen. Such a complex formation between superoxide ion and metal ions has been shown to play an essential role in the enzymatic function of superoxide dismutase, formation of active oxygen–copper complexes and the novel catalytic effect of O_2 in back electron transfer of zinc porphyrin–fullerene linked molecules.

Keywords: Superoxide ion; Metal ion; Superoxide dismutase; Catalysis; Back electron transfer

1. Introduction

Redox-active metal ions in particular transition-metal ions exhibit characteristic coordination environments depending on their oxidation states and their redox reactivities are finely controlled by the ligands coordinating to the metals [1–3]. Redox-inactive metal ions which can act as Lewis acids have also played a pivotal role in promoting various reactions of synthetic value because of the high reactivities and selectivities achieved under mild reaction conditions [4–8]. On the other hand, the biological catalytic activity of metalloproteins for redox reactions is usually associated with a particular coordination environment of the metal active site [9,10]. There has been particular interest in O_2-binding and -activation by non-heme metalloenzymes [11–16]. A redox-active metal center is often associated with another metal center which can accelerate the redox process of O_2 in biological systems [9,10]. An important

* Corresponding author. Tel.: +81-6-6879-7368; fax: +81-6-6879-7370.

E-mail address: fuzukumi@chem.eng.osaka-u.ac.jp (S. Fukuzumi).

0010-8545/02/$ - see front matter
PII: S0010-8545(01)00435-0

example of such systems is the copper, zinc superoxide dismutase (Cu,Zn-SOD) which contains an imidazolate-bridged Cu(II)–Zn(II) bimetallic center in its active site [17–20]. The Cu,Zn-SOD enzyme catalyzes the disproportionation (dismutation) of toxic $O_2^{\bullet -}$ to O_2 and H_2O_2, [21,22] thus preventing oxidative damage by the anticancer and antiaging mechanisms [23,24]. The copper ion is coordinated to four imidazole N atoms of histidine residues in a distorted square-pyramidal geometry while the zinc ion located at a distance of 6.2 Å from the copper ion is coordinated to a carboxylato O atom of an aspartic acid residue and three imidazole N atoms of histidine residues in a distorted tetrahedral structure [17,18]. A number of SOD model complexes have been designed and synthesized to provide valuable insights into the structure and catalytic function of the Cu,Zn-SOD active site [25–31]. The most important question to be answered is how the Cu,Zn-SOD active site can accelerate both the oxidation and reduction of $O_2^{\bullet -}$, required for the rapid disproportionation. Such a dual role would be made possible by the bimetallic system, since any monometallic system can only activate either the oxidation or reduction of $O_2^{\bullet -}$. One metal site can act as a redox-active site and the other acts as a Lewis acid to control the redox reaction.

This review is intended to focus on such a dual role of metal ions on the catalytic control of redox reactions

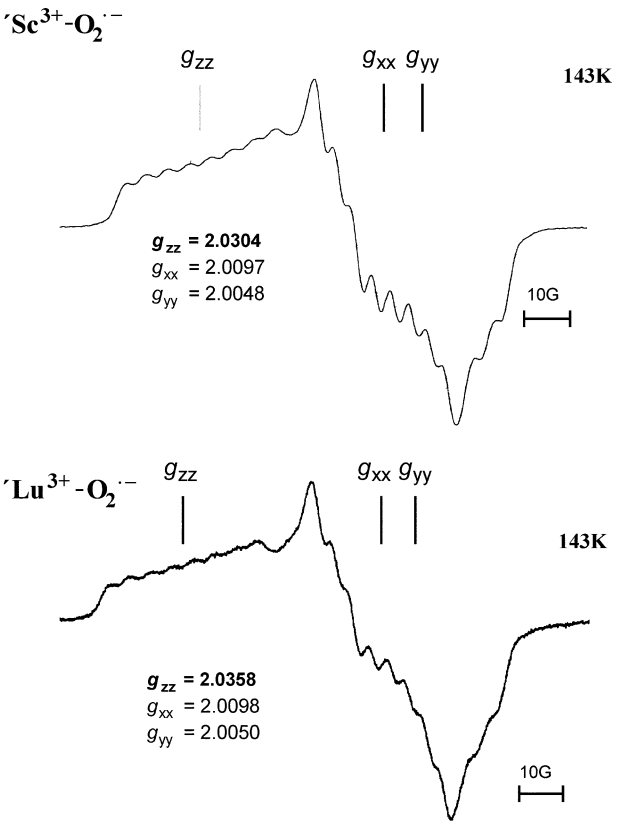

Fig. 1. EPR spectra of $O_2^{\bullet -}$–Sc^{3+} and $O_2^{\bullet -}$–Lu^{3+} complexes at 143 K [33].

of O_2. The catalytic reactivities of metal ions are certainly related to the Lewis acidity of metal ions employed to promote the redox reactions via binding of metal ions with $O_2^{\bullet -}$. Charges and ion radii are important factors to determine the Lewis acidity of metal ions. We begin with a quantitative measure to determine the Lewis acidity of a variety of metal ions introduced in relation to the catalytic reactivities of metal ions in the electron transfer reduction of O_2. How both the oxidation and reduction of $O_2^{\bullet -}$ can be accelerated by bimetallic systems is discussed in relation with the SOD and oxygen activation mechanisms. Finally a recent finding that O_2 can act as a novel catalyst to accelerate back electron transfer (BET) reactions of artificial photosynthetic reaction centers is presented to demonstrate the importance of binding of metal ions to $O_2^{\bullet -}$ in controlling electron transfer reactions [32].

2. Quantitative measure of the Lewis acidity of metal ions

It is difficult to know the difference in the Lewis acidity of a variety of metal ions (M^{n+}) in a quantitative manner. However, it has recently been shown that the binding energies of a variety of metal ions with superoxide ion ($O_2^{\bullet -}$) can be readily derived from the g_{zz}-values of the EPR spectra of the superoxide–metal ion complexes ($O_2^{\bullet -}$–M^{n+}), providing a quantitative measure of the Lewis acidity of the metal ions as follows [33].

A variety of metal ions (M^{n+}) can form complexes with $O_2^{\bullet -}$ [33,34]. The $O_2^{\bullet -}$–M^{n+} complexes can be produced by photoinduced electron transfer from the excited state of dimeric 1-benzyl-1,4-dihydronicotinamide [$(BNA)_2$], which can act as a unique two electron donor [35,36], to O_2 in the presence of a metal ion in acetonitrile (Eq. (1)) [33]. The addition of scandium triflate ($Sc(OTf)_3$) or lutetium triflate ($Lu(OTf)_3$) to the $(BNA)_2$–O_2 system results in the appearance of the anisotropic EPR signal after irradiation by light as shown in Fig. 1 [33]. The eight-line superhyperfine coupling of $O_2^{\bullet -}$ with the 7/2 nuclear spin of the scandium or lutetium nucleus is seen around each g component in the anisotropic signal, demonstrating the spin delocalization to the scandium or lutetium nucleus due to the complexation of metal ion with $O_2^{\bullet -}$. The isotropic g value (2.0163) is appreciably smaller than the average value (2.030) [37] of the principal three g components of $O_2^{\bullet -}$ at 77 K.

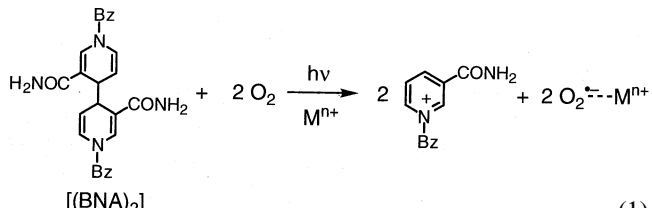

(1)

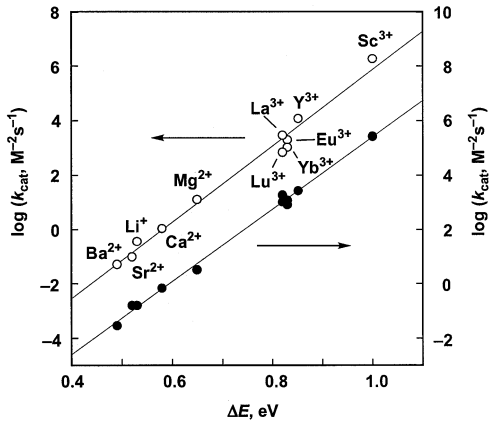

Fig. 2. Plots of log k_{cat} vs. ΔE in M^{n+}-catalyzed electron transfer from (TPP)Co to O_2 (○) and *p*-benzoquinone (●) in acetonitrile at 298 K [33].

Oxygen enriched in ^{17}O gave the EPR spectrum of the $O_2^{\bullet-}$–Sc^{3+} complex with ^{17}O enriched oxygen, in which two inequivalent a(^{17}O) values (21 and 14 G) were obtained [34]. Such inequivalent $a(^{17}O)$ values are fully consistent with an 'end-on' coordination of $^{\bullet}O$–O^-–Sc^{3+} in which the electron spin is more localized at the terminal oxygen. The unrestricted Hartree–Fock (UHF) SCF optimization using the 6-311 + + G** basis set also supports an 'end-on' coordination form of $^{\bullet}O$–O^-–Sc^{3+} [34]. When $O_2^{\bullet-}$ is adsorbed on solid surfaces, both side-on and end-on coordinations have been reported depending on metal oxides [38–41].

A variety of metal ions (M^{n+}) form $O_2^{\bullet-}$ complexes and exhibit EPR spectra where the g_{zz}-value varies depending on the type of metal ion. The g_{zz}-value of $O_2^{\bullet-}$–M^{n+} provides valuable information concerning the binding strength of $O_2^{\bullet-}$–M^{n+}. The deviation of the g_{zz}-value from the free spin value ($g_e = 2.0023$) is caused by the spin–orbit interaction as given by Eq. (2) [42],

$$g_{zz} = g_e + 2\sqrt{\frac{\lambda^2}{\lambda^2 + \Delta E^2}} \quad (2)$$

where λ is the spin–orbit coupling constant (0.014 eV) [43] and ΔE is the energy splitting of π_g levels due to complex formation between $O_2^{\bullet-}$ and M^{n+}. Under the conditions that $\Delta E \gg \lambda$, Eq. (2) is rewritten as Eq. (3)

$$\Delta E = 2\lambda/(g_{zz} - g_e) \quad (3)$$

in which the ΔE value is readily obtained from the deviation of the g_{zz}-value from the free spin value. The ΔE value, commonly in the range 0.3–1.0 eV increases generally in order: monovalent cations (M^+) < divalent cations (M^{2+}) < trivalent cations (M^{3+}) [33]. The ΔE value also increases with decreasing the ion radius when the oxidation state of the metal ion is the same. The same trend has been reported for $O_2^{\bullet-}$ adsorbed on the surface of various metal oxides [44]. Scandium ion which has the smallest ion radius among the trivalent metal cations gives the largest ΔE value, and this indicates that the binding energy between Sc^{3+} and $O_2^{\bullet-}$ is the strongest [33]. The calculated O–O distance decreases in the order: $O_2^{\bullet-}$ (1.343 Å) > $O_2^{\bullet-}$–Li^+ (1.309 Å) > $O_2^{\bullet-}$–Mg^{2+} (1.297 Å) > $O_2^{\bullet-}$–Sc^{3+} (1.211 Å) as the ΔE value increases [33].

The applicability of ΔE to predict the catalytic reactivities of M^{n+} in electron transfer reactions has nicely been shown in M^{n+}-catalyzed electron transfer from (TPP)Co (TPP = tetraphenylporphyrin dianion) to O_2 (Eq. (4)) in acetonitrile at 298 K [33,45].

$$(TPP)Co + O_2 \xrightarrow[k_{cat}]{M^{n+}} [(TPP)Co]^+ + O_2^{\bullet-}\text{–}M^{n+} \quad (4)$$

In the absence of metal ion, no electron transfer from (TPP)Co to O_2 occurs since the electron transfer is highly endergonic judging from the one-electron oxidation potential of (TPP)Co ($E^\circ_{ox} = 0.35$ V vs. SCE in MeCN) [46] and the one-electron reduction potential of O_2 ($E^\circ_{red} = -0.87$ V vs. SCE) [47]. The catalytic effects of metal ions in electron transfer reduction of substrates have been ascribed to the binding of metal ions to the radical anions produced in the electron transfer reactions [48,49]. There is a *striking linear correlation* between the catalytic rate constants (log k_{cat}) of electron transfer from (TPP)Co to O_2 and ΔE of $O_2^{\bullet-}$–M^{n+} derived from the g_{zz}-values as shown in Fig. 2 (open circles). The remarkable correlation spans a range of almost 10^7 in the rate constant. The slope of the linear correlation between log k_{cat} for M^{n+}-catalyzed electron transfer from (TPP)Co to O_2 and ΔE is obtained as 14.0 eV^{-1} which is close to the value of $1/2.3kT$ ($= 16.9$ eV^{-1}, where k is the Boltzmann constant and $T = 298$ K). Such a correlation has also been observed for the M^{n+}-catalyzed electron transfer from (TPP)Co to *p*-benzoquinone (Q) as shown in Fig. 2 (open circles) [33]. The slope (13.3) for Q is nearly the same as the slope (14.0) for O_2. This means that the variation of ΔE is well reflected in the difference in the activation free energy for the M^{n+}-promoted electron transfer from (TPP)Co to Q as well as O_2. The stronger the binding of M^{n+} with $O_2^{\bullet-}$, the larger will be the catalytic effects of M^{n+}. Thus, ΔE is regarded as a good measure of the binding energies in the $O_2^{\bullet-}$–M^{n+} complexes, which can be used as a quantitative measure of Lewis acidity of the metal ion.

3. Catalytic mechanism of SOD

Cu,Zn-SOD protects cells against oxidative damage by catalyzing the disproportionation (dismutation) of toxic $O_2^{\bullet-}$ to O_2 and H_2O_2 [17–20,50]. The important role of Zn(II) ion in the bimetallic system to activate both the oxidation and reduction of $O_2^{\bullet-}$ has been

implicated by a well-characterized SOD model, that is an imidazolate-bridged Cu(II)–Zn(II) heterodinuclear complex containing a dinucleating ligand, Hbdpi (Hbdpi = 4,5-bis(di(2-pyridylmethyl)aminomethyl)-imidazole) [31]. The crystal structure is shown in Fig. 3 [31]. The Cu(II)–Zn(II) distance of 6.197(2) Å in the Cu(II)–Zn(II) heterodinuclear complex agrees well with that of native Cu,Zn-SOD (6.2 Å), and each metal has the pentacoordinate geometry with the imidazolate nitrogen, two pyridine nitrogens, the tertiary amine nitrogen and a solvent (MeCN or H_2O) [31]. The ESR spectrum of complex of the Cu(II)–Zn(II) heterodinuclear complex gave the well-defined ESR parameters

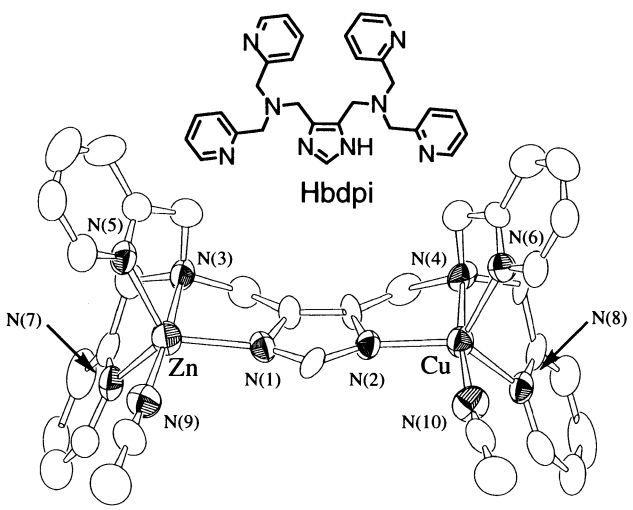

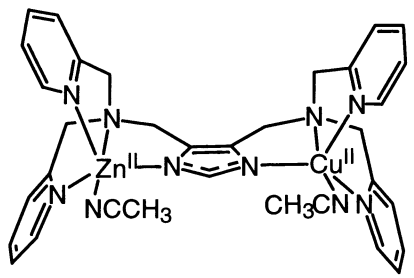

$[CuZn(bdpi)(CH_3CN)_2](ClO_4)_3 \cdot 2CH_3CN$

Fig. 3. ORTEP view of $[Cu^{II}Zn^{II}(bdpi)(CH_3CN)_2](ClO_4)_3 \cdot 2CH_3CN$ [42]. The hydrogen atoms are omitted for clarity.

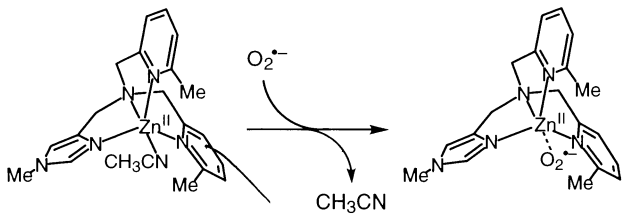

$[Zn^{II}(MeIm(Me)_2)(CH_3CN)]^{2+}$

Scheme 1.

($g_{\|} = 2.10$, $g_{\perp} = 2.24$, $|A_{\|}| = 11.7$ mT and $|A_{\perp}| = 12.4$ mT), which indicate that the Cu(II) ion in the complex has a trigonal bipyramidal environment and a d_z2 ground state following the criteria given by Bencini et al. [51], in agreement with the X-ray structure in Fig. 3 [31]. The observation of well-defined ESR spectrum also confirms that the complex retains its imidazolate-bridged Cu(II)–Zn(II) heterodinuclear structure and that it is not a 1:1 mixture of Cu(II)–Cu(II) and Zn(II)–Zn(II) homodinuclear complexes. The Cu(II)–Zn(II) SOD model complex which has a coordination site available for the binding of superoxide as shown in Fig. 3 exhibits the highest activity among the structurally established SOD models reported so far [30,31].

A large positive shift (about 0.2 V) in the $E_{1/2}$ value of the Cu(II)–Zn(II) complex is observed as compared to the corresponding Cu(II) mononuclear complexes [31]. This indicates that an important role of Zn(II) ion in the imidazolate-bridged Cu(II)–Zn(II) complex is to accelerate an outer-sphere electron transfer from $O_2^{\bullet -}$ to produce the Cu(I)–Zn(II) complex, when the free energy change of electron transfer becomes thermodynamically more favorable as compared to that without Zn(II) ion. The presence of Zn(II) which can act as a Lewis acid is also able to accelerate an electron transfer from the Cu(I)–Zn(II) complex to $O_2^{\bullet -}$, since $O_2^{\bullet -}$ can form a complex with metal ions acting as a Lewis acid to accelerate the electron transfer reduction of $O_2^{\bullet -}$ (vide supra) [33]. Such an acceleration for the reduction of $O_2^{\bullet -}$ can also be attained by a Brønsted acid instead of a Lewis acid since Valentine and coworkers reported that the reduction of $O_2^{\bullet -}$ for the zinc-deficient SOD form is acid-catalyzed [52]. The formation of $O_2^{\bullet -}$–Zn(II) complex is confirmed using Zn(II) complexes, $[Zn^{II}(MeIm(Py)_2)(CH_3CN)](ClO_4)_2$ and $[Zn^{II}(MeIm(Me)_2)(CH_3CN)](ClO_4)_2$ ($MeIm(Me)_2$ = (1-methyl-4-imidazolylmethyl)bis(6-methyl-2-pyridylmethyl)amine), as shown in Scheme 1 [53]. The ESR spectra of the Zn(II)–$O_2^{\bullet -}$ complexes measured at 133 K gave the g_{zz}-values which are significantly smaller than the value of free $O_2^{\bullet -}$ due to the complexation of Zn(II) ion with $O_2^{\bullet -}$ [53]. The ΔE values of the Zn(II)–$O_2^{\bullet -}$ complexes have been evaluated from a deviation of the g_{zz}-values from the free spin value. The ΔE values of the $O_2^{\bullet -}$ complex with $[Zn^{II}(MeIm(Me)_2Py]^{2+}$ (0.87 eV) and $[Zn^{II}(MeIm(Py)_2)]^{2+}$ (0.85 eV) are significantly larger than those of $O_2^{\bullet -}$ complexes with other divalent metal ions (Mg(II) ion: 0.65 eV, Ca(II) ion: 0.58 eV, Sr(II) ion: 0.52 eV and Ba(II) ion: 0.49 eV) [33], reflecting the strong Lewis acidity of Zn(II) ion as compared to other divalent metal ions [53]. The larger ΔE value of the $O_2^{\bullet -}$ complex with $[Zn^{II}(MeIm(Me)_2Py]^{2+}$ as compared to $[Zn^{II}(MeIm(Py)_2)]^{2+}$ (0.85 eV) may be ascribed to the increased Lewis acidity of the Zn(II) ion in $[Zn^{II}(MeIm(Me)_2Py]^{2+}$ due to the steric effect of the *o*-methyl group of pyridine moiety of

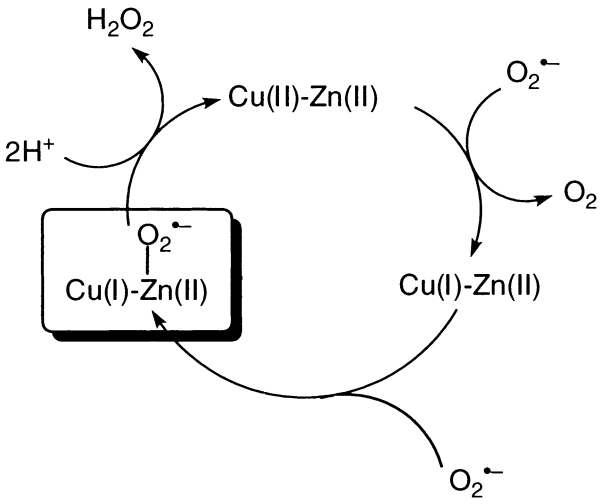

Scheme 2.

$[Zn^{II}(MeIm(Me)_2Py]^{2+}$ [52]. Thus, the essential role of Zn(II) ion in SODs is to accelerate both the oxidation and reduction of superoxide by controlling the redox potentials of Cu(II) ion and superoxide in the catalytic cycle of SOD as shown in Scheme 2 [31]. A similar effect is also expected for another copper ion in the Cu(II)–Cu(II) homodinuclear complex containing the same Hbdpi ligand [31]. The same mechanism as Scheme 2 can be applied to the disproportionation of semiquinone radical anion by the imidazolate-bridged Cu(II)–Zn(II) complex [54]. The Zn(II) ion also plays the essential role in facilitating the reduction of semiquinone radical anion by coordination of the radical anion to the Zn(II) ion [54].

4. Formation of active oxygen–metal complexes

The binding of $O_2^{\bullet -}$ to Cu(II) ion can facilitate the further reduction of $O_2^{\bullet -}$ by Cu(I) ion to O_2^{2-} to give a (μ-η^2:η^2-peroxo)dicopper(II) complex [11,55], which has been confirmed to exist in the enzyme active site of oxyhemocyanin [56,57]. The reaction of $[Cu^{I}L](PF_6)$ (L = *N*,*N*-bis[2-(2-pyridyl)ethyl]-2-phenylethylamine) with O_2 in THF at −80 °C was reported to give the (μ-η^2:η^2-peroxo)dicopper(II) complex, $[Cu^{II}_2(O^2_2)L_2](PF_6)_2$, the formation of which was confirmed by the spectroscopic analyses [58,59]. The kinetic study on formation of the peroxo complex indicates that the reaction of the Cu(I) complex and the monomeric superoxocopper(II) complex is rate-determining as shown in Scheme 3 [59]. A superoxocopper(II) complex with a sterically hindered ligand which can prevent the formation of the (μ-η^2:η^2-peroxo)dicopper(II) complex was isolated and the X-ray structure was determined to show a side-on binding of $O_2^{\bullet -}$ and the Cu(II) ion [60].

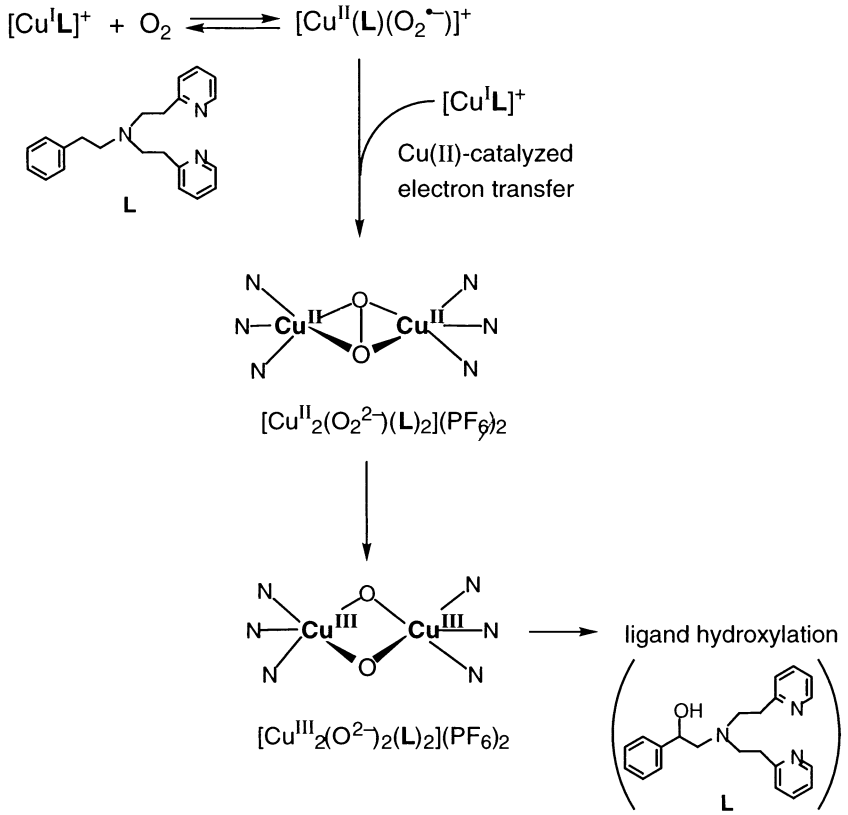

Scheme 3.

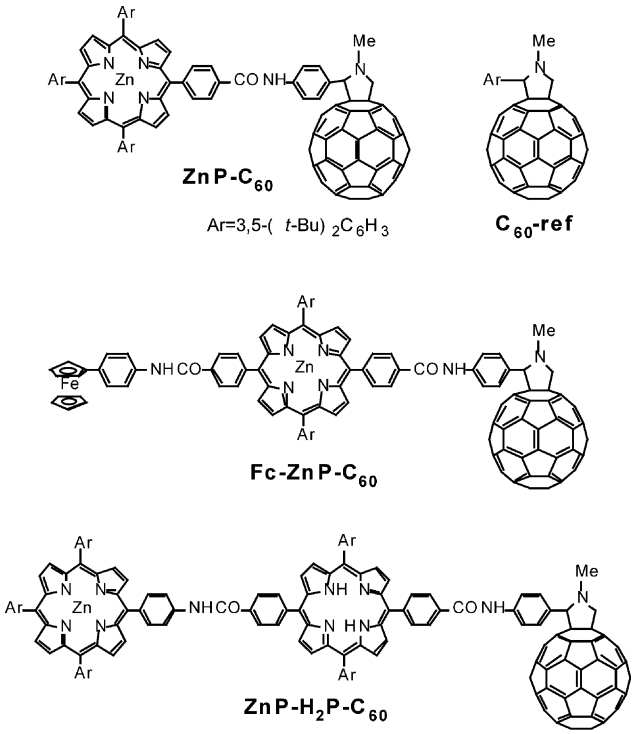

Fig. 4. Structures of zinc porphyrin–fullerene linked compounds.

The strong interaction between $O_2^{\bullet-}$ and the Cu(II) ion makes it possible to further reduce $O_2^{\bullet-}$ to O_2^{2-} by another $[Cu^{I}L]^{+}$, leading to the formation of the (μ-η^2:η^2-peroxo)dicopper(II) complex (Scheme 3). However, the change in the one-electron reduction potential of $O_2^{\bullet-}$ by the binding to the Cu(II) ion has yet to be determined.

The further intramolecular electron transfer from the two Cu(II) ions to O_2^{2-} in the (μ-η^2:η^2-peroxo)dicopper(II) complex may result in the O–O bond cleavage to give the bis(μ-oxo)dicopper(III) complex which is suggested to be the actual reactive intermediate for the efficient benzylic ligand hydroxylation as shown in Scheme 3 [59]. Interconversion between the (μ-η^2:η^2-peroxo)dicopper(II) complex and the bis(μ-oxo)dicopper(III) complex was observed using the *i*-Pr_3TACN ligand (*i*-Pr_3 TACN = 1,4,7-triisopropyl-1,4,7-triazacyclononane) just by changing the solvent between CH_2Cl_2 and THF, where the oxidative *N*-dealkylation occurs efficiently from the bis(μ-oxo)dicopper(III) complex [61,62]. Thus, these two forms of the active oxygen dicopper complex may be similar in their energies.

5. Catalysis of O_2 in electron transfer via coordination to Zn(II) ion

Coordination of $O_2^{\bullet-}$ to Zn(II) ion plays an important role not only in the catalytic function of Cu,Zn-SOD (Scheme 2) but also in the novel catalytic effect of O_2 in BET from a fullerene radical anion to a zinc porphyrin moiety within photolytically generated radical ion pairs of zinc porphyrin–fullerene linked molecules shown in Fig. 4 [32]. This is the first example in which O_2, the most important biological oxidant, acts as a catalyst rather than an oxidant in BET reactions.

These zinc porphyrin–fullerene linked dyad and triads have been developed as artificial photosynthetic systems which, upon photoexcitation, give rise to long-lived charge-separated states in high quantum yields [63]. The energy levels in benzonitrile are shown in Scheme 4 to illustrate the different relaxation pathways of photoexcited ZnP–C_{60} [63]. The charge-separated state is obtained from the photoinduced electron transfer involving the singlet and triplet excited states of ZnP and C_{60} and decays via the back electron transfer from $C_{60}^{\bullet-}$ to $ZnP^{\bullet+}$. Each step in Scheme 4 can be monitored by time-resolved techniques, including fluorescence lifetime and transient absorption measurements, disclosing the crucial formation of $ZnP^{\bullet+}$-*spacer*-$C_{60}^{\bullet-}$ and Fc^{+}-*spacer*-$C_{60}^{\bullet-}$ pairs in a variety of solvents [63].

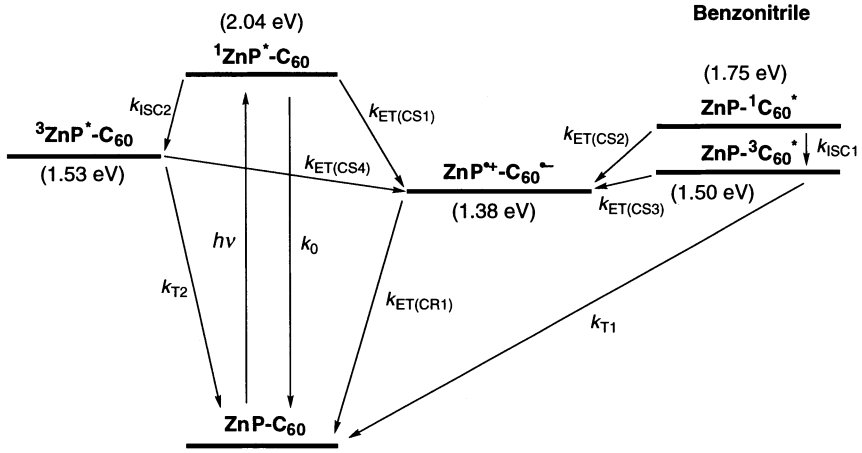

Scheme 4.

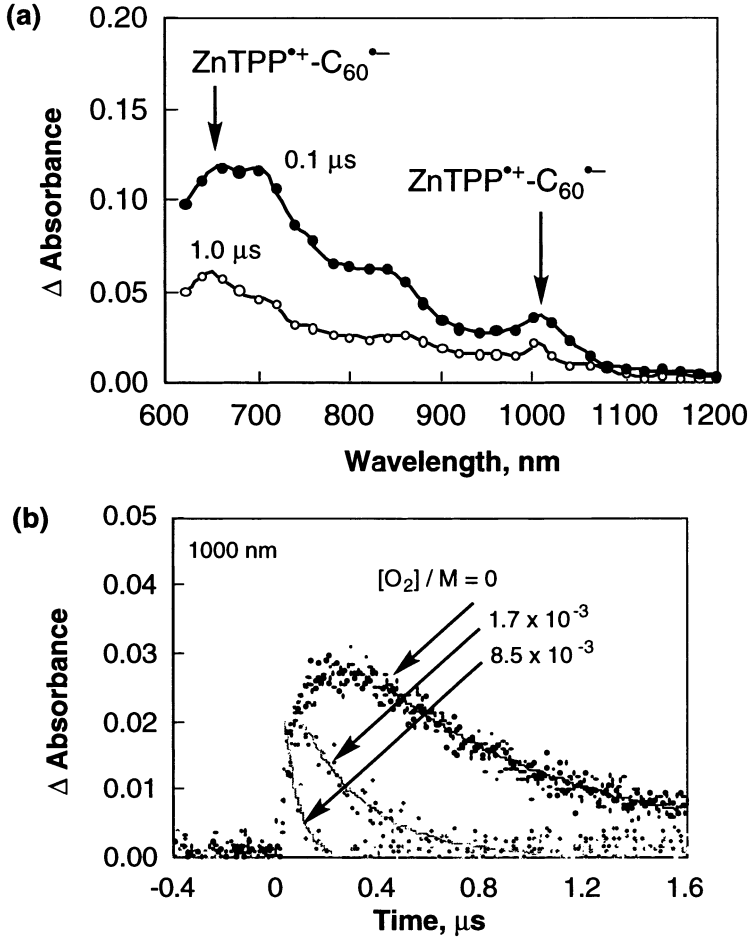

Fig. 5. (a) Transient absorption spectra for ZnP–C_{60} 0.10 and 1.0 μs after laser excitation in the absence and presence of O_2 in PhCN [32]. (b) Time profiles of the absorbance at 1000 nm due to $C_{60}^{\bullet-}$ in $ZnP^{\bullet+}$–$C_{60}^{\bullet-}$ [32].

Table 1
Rate constants k_{BET} for back electron transfer and the free energy change ($-\Delta G^{\circ}_{BET}$) [a] in fullerene-based dyad and triads in the absence and presence of O_2 in PhCN [32]

Compound	k_{BET} (s^{-1})			
	$-\Delta G^{\circ}_{BET}$ (eV)	$[O_2] = 0$ M	1.7×10^{3} M	8.6×10^{3} M
$ZnP^{\bullet+}$–$C_{60}^{\bullet-}$	1.38	1.3×10^{6}	3.8×106	1.5×10^{7}
$ZnP^{\bullet+}$–H_2P–$C_{60}^{\bullet-}$	1.34	3.7×10^{4}	1.1×10^{5} (1.2×10^{5}) [b]	3.2×10^{5}
Fc^{+}–ZnP–$C_{60}^{\bullet-}$	1.03	1.2×10^{5}	1.3×10^{5}	1.3×10^{5}

[a] The $-\Delta G_{BET}$ values are obtained from difference between the one-electron oxidation and reduction potentials which are determined by differential pulse voltammetry in PhCN containing 0.1 M Bu_4NPF_6.
[b] $[O_2] = 2.6\times10^{-3}$ M.

For example, a deoxygenated benzonitrile (PhCN) solution containing ZnP–C_{60} gives rise upon a 532 nm laser pulse to a characteristic absorption spectrum with maxima at 650 and at 1000 nm (Fig. 5a) [32]. While the former maximum (i.e. 650 nm) is a clear attribute of the $ZnP^{\bullet+}$ [64], the latter maximum (i.e. 1000 nm) corresponds to the diagnostic marker of the fullerene radical anion [65]. The decay of both absorption bands obeys clear first-order kinetics. This indicates an intramolecular BET from $C_{60}^{\bullet-}$ to $ZnP^{\bullet+}$ governs the fate of the $ZnP^{\bullet+}$–$C_{60}^{\bullet-}$ radical ion pair. In the presence of O_2, the decay rate of both $C_{60}^{\bullet-}$ and $ZnP^{\bullet+}$ absorption is markedly accelerated as compared to that found in the absence of O_2 (Fig. 5b). The decay rate of $C_{60}^{\bullet-}$ coincides with that of $ZnP^{\bullet+}$ and, in addition, increases linearly with increasing O_2 concentration. The rate constants (k_{BET}) in the absence and presence of O_2 for a series of ZnP–C_{60} linked systems in PhCN are summarized in Table 1.

In contrast to the ZnP–C_{60} dyad, the k_{BET} from $C_{60}^{\bullet-}$ to ferrocenium ion (Fc^{+}) in Fc^{+}–ZnP–$C_{60}^{\bullet-}$ under O_2-saturated conditions matches surprisingly the value determined in the absence of O_2 (Table 1). The smaller k_{BET} value of the triad (Fc–ZnP–C_{60}: 1.3×10^{5} s^{-1}) as compared to that of the dyad (ZnP–C_{60}: $1.3\times$

10^6 s^{-1}) stems from the larger edge-to-edge distance of the former ($R_{ee} = 30.3$ Å) [66] relative to the latter ($R_{ee} = 11.9$ Å) [67,68]. Although an even smaller k_{BET} value (4.8×10^4 s^{-1}) was noted for the BET dynamics from $C_{60}^{\bullet-}$ to $ZnP^{\bullet+}$ in the $ZnP^{\bullet+}$–H_2P–$C_{60}^{\bullet-}$ triad, the k_{BET} value is, nevertheless, expedited with increasing O_2 concentration as shown in Table 1. Thus, the presence of $ZnP^{\bullet+}$ appears, without any doubt, essential for the accelerating effect of O_2 on the decay of the radical ion pair. The energy transfer pathway from $ZnP^{\bullet+}$–$C_{60}^{\bullet-}$ via ZnP–$^3C_{60}^*$ has been ruled out as a major contributor to the decay of the radical ion pair, since much smaller intensity of $^1\Delta_g$ O_2 phosphorescence of the ZnP–C_{60} system is observed as compared to C_{60} [32].

The electron transfer from $C_{60}^{\bullet-}$ to O_2 is endergonic [$\Delta G_{et}^\circ \gg 0$ (0.28 eV)], judging from the one-electron reduction potentials of both species: E_{red}° of O_2 (-1.33 V vs. Fc/Fc^+) is significantly lower than that of C_{60} (-1.05 V vs. Fc/Fc^+) [32]. Thus, a direct electron transfer from $C_{60}^{\bullet-}$ in $ZnP^{\bullet+}$–$C_{60}^{\bullet-}$ to O_2 is highly unlikely to occur in benzonitrile. In addition, the concomitant decay of $ZnP^{\bullet+}$ and $C_{60}^{\bullet-}$ in Fig. 5a is inconsistent with a direct electron transfer from $C_{60}^{\bullet-}$ to O_2, which would yield stable $ZnP^{\bullet+}$–C_{60} and $O_2^{\bullet-}$ on the present time scale. The catalytic participation of O_2 in an intramolecular BET between $C_{60}^{\bullet-}$ and $ZnP^{\bullet+}$ in ZnP-linked C_{60} is depicted in Schemes 5 and 6. The intermolecular ET from $C_{60}^{\bullet-}$ to O_2 may be initiated by the coordination of O_2 to $ZnP^{\bullet+}$, followed by electron transfer from $C_{60}^{\bullet-}$ to O_2 coordinated to $ZnP^{\bullet+}$ to yield $O_2^{\bullet-}$ bound to $ZnP^{\bullet+}$. Due to the strong binding

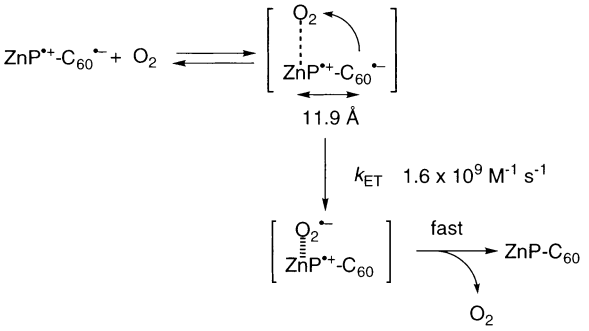

Scheme 5.

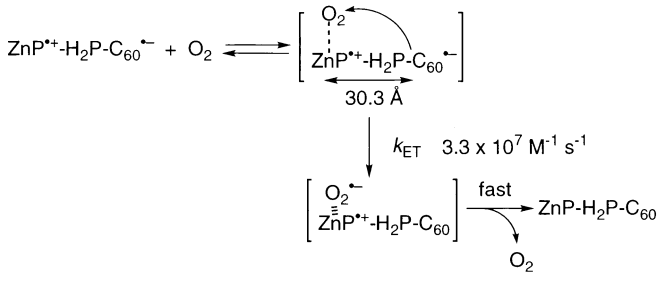

Scheme 6.

of $O_2^{\bullet-}$ to $ZnP^{\bullet+}$, the one-electron reduction potential of O_2 is shifted towards positive values, namely, in favor of the ET event. The complexation is then followed by a rapid intramolecular ET from $O_2^{\bullet-}$ to $ZnP^{\bullet+}$ in the $O_2^{\bullet-}$–$ZnP^{\bullet+}$ complex to regenerate O_2 (Scheme 5). In the presence of metal ions, $O_2^{\bullet-}$ is known to coordinate to the metal ion, yielding the corresponding $O_2^{\bullet-}$–metal ion complex as described above [33]. The binding energy of $O_2^{\bullet-}$ with Zn(II) ion (ca. 0.9 eV) [53] is sufficient to make an electron transfer from $C_{60}^{\bullet-}$ to O_2 energetically feasible. In contrast to the ZnP containing donor–acceptor systems, ferrocene is a fully coordinated complex, omitting the coordination of another ligand, such as $O_2^{\bullet-}$. As a matter of fact, this seems the likely rationale for the lack of accelerating effects in the Fc^+–ZnP–$C_{60}^{\bullet-}$ system.

The second-order rate constant of $ZnP^{\bullet+}$–$C_{60}^{\bullet-}$ (1.6×10^9 M^{-1} s^{-1}) obtained from the linear dependence of k_{BET} on [O_2] in PhCN is only slightly lower than the diffusion-controlled limit in PhCN (5.6×10^9 M^{-1} s^{-1}). On the other hand, the corresponding value of $ZnP^{\bullet+}$–H_2P–$C_{60}^{\bullet-}$ (3.3×10^7 M^{-1} s^{-1}) is 48 times smaller as compared to the value of $ZnP^{\bullet+}$–$C_{60}^{\bullet-}$. Such a decreased rate for $ZnP^{\bullet+}$–H_2P–$C_{60}^{\bullet-}$ as compared to $ZnP^{\bullet+}$–$C_{60}^{\bullet-}$ is also inconsistent with the energy transfer pathway, since the triplet energy of $^3C_{60}^*$ is essentially the same between ZnP–$^3C_{60}^*$ and ZnP–H_2P–$^3C_{60}^*$. Remarkably, this k_{ET}-ratio (48) is consistent with the k_{BET}-ratio (27) (i.e. from $C_{60}^{\bullet-}$ to $ZnP^{\bullet+}$) between the triad and the dyad, however, in the absence of O_2. Thus, ET from $ZnP^{\bullet+}$–H_2P–$C_{60}^{\bullet-}$ to O_2 occurs even at the longer distance as compared to ET from $ZnP^{\bullet+}$–$C_{60}^{\bullet-}$ dyad, since O_2 is placed at a longer distance from $C_{60}^{\bullet-}$ in the precursor complex for the electron transfer from $C_{60}^{\bullet-}$ to O_2 in $ZnP^{\bullet+}$–H_2P–$C_{60}^{\bullet-}$ (see Scheme 6 as compared to Scheme 5). In this way, O_2 acts as a novel *catalyst* to expedite intramolecular BET in ZnP-linked C_{60} systems where $ZnP^{\bullet+}$ accelerates the reaction of $C_{60}^{\bullet-}$ with O_2 and, in turn, activates the catalysis of O_2 in the overall BET from $C_{60}^{\bullet-}$ to $ZnP^{\bullet+}$ (Schemes 5 and 6).

6. Summary

In this minireview article, we have demonstrated that coordination of $O_2^{\bullet-}$ to metal ions plays an important role in controlling the redox reactivity of O_2 not only in the electron transfer reduction of O_2 and $O_2^{\bullet-}$ but also in the novel catalytic effect of O_2 in back electron transfer reaction involving the Zn(II) ion which can act as a Lewis acid. The binding energies of $O_2^{\bullet-}$ with metal ions derived from the g_{zz}-values of the EPR spectra of $O_2^{\bullet-}$–metal ion complexes provide a quantitative measure of the Lewis acidity of the metal ions in

predicting the catalytic reactivities of metal ions in electron transfer reactions of O_2 and other substrates.

Acknowledgements

The authors are deeply indebted to the work of all collaborators and coworkers whose names are listed in the references. S.F. acknowledges continuous support of the Ministry of Education, Science, Culture and Sports, Japan (a Grant-in-Aid for Scientific Research Priority Area, No. 11228205).

References

[1] H. Taube, Electron Transfer Reactions of Complex Ions in Solution, Academic Press, New York, 1970.
[2] D. Astruc, Electron Transfer and Radical Processes in Transition Metal Chemistry, VCH, New York, 1995.
[3] A. Vlcek Jr., in: V. Balzani (Ed.), Electron Transfer in Chemistry, vol. 2, Wiley–VCH, Weinheim, 2001, p. 5 (chap. 5).
[4] H. Yamamoto, Lewis Acid Chemistry: A Practical Approach, Oxford University Press, Oxford, 1999.
[5] D. Schinzer (Ed.), Selectivities in Lewis Acid Promoted Reactions, Kluwer Academic, Dordrecht, 1989.
[6] M. Santelli, J.-M. Pons, Lewis Acids and Selectivity in Organic Synthesis, CRC Press, Boca Raton, FL, 1995.
[7] P. Singh, Chem. Rev. 97 (1997) 721.
[8] R. Mahrwald, Chem. Rev. 99 (1999) 1095.
[9] W. Kaim, B. Schwederski, Bioinorganic Chemistry: Inorganic Elements in the Chemistry of Life, Wiley, New York, 1991.
[10] S.J. Lippard, Science 261 (1993) 699.
[11] N. Kitajima, Y. Moro-oka, Chem. Rev. 94 (1994) 737.
[12] S. Fox, K.D. Karlin, in: J.S. Valentine, C.S. Foote, A. Greenberg, J.F. Liebman (Eds.), Active Oxygen in Biochemistry, Chapman and Hall, London, 1995, pp. 188–231.
[13] L. Que Jr., in: J.S. Valentine, C.S. Foote, A. Greenberg, J.F. Liebman (Eds.), Active Oxygen in Biochemistry, Chapman and Hall, London, 1995, pp. 232–275.
[14] A.L. Feig, S.J. Lippard, Chem. Rev. 94 (1994) 759.
[15] E.I. Solomon, F. Tuczek, D.E. Root, C.A. Brown, Chem. Rev. 94 (1994) 827.
[16] L. Que Jr., R.Y.N. Ho, Chem. Rev. 96 (1996) 2607.
[17] I. Fridovich, J. Biol. Chem. 264 (1989) 7761.
[18] I. Bertini, L. Banci, M. Piccioli, Coord. Chem. Rev. 100 (1990) 67.
[19] J.A. Tainer, E.D. Getzoff, J.S. Richardson, D.C. Richardson, Nature 306 (1983) 284.
[20] A.E.G. Cass, in: P. Harrison (Ed.), Superoxide Dismutases in Metalloproteins, Part 1, Chemie, Weinheim, 1985, p. 121.
[21] E.M. Fielden, P.B. Roberts, R.C. Bray, D.J. Lowe, G.N. Mautner, G. Rotilio, L. Calabrese, J. Biochem. 139 (1974) 49.
[22] L.M. Ellerby, D.E. Cabelli, J.A. Graden, J.S. Valentine, J. Am. Chem. Soc. 118 (1996) 6556.
[23] L.W. Oberley, G.R. Buettner, Cancer Res. 39 (1979) 1141.
[24] K.J. Farmer, R.S. Sohal, Free Radical Biol. Med. 7 (1989) 23.
[25] G. Kolks, C.R. Frihart, H.N. Rabinowitz, S.J. Lippard, J. Am. Chem. Soc. 98 (1976) 5720.
[26] K.G. Strotkamp, S.J. Lippard, Acc. Chem. Res. 15 (1982) 318.
[27] B.P. Murphy, Coord. Chem. Rev. 124 (1993) 63.
[28] A. Gartner, U. Weser, Top. Curr. Chem. 132 (1986) 1.
[29] C.A. Salata, M.T. Youinou, C.J. Burrows, J. Am. Chem. Soc. 111 (1989) 9278.
[30] J.-L. Pierre, P. Chautemps, S. Refaif, C. Beguin, A.E. Marzouki, G. Serratrice, E. Saint-Aman, P. Rey, J. Am. Chem. Soc. 117 (1995) 1965.
[31] H. Ohtsu, Y. Shimazaki, A. Odani, O. Yamauchi, W. Mori, S. Itoh, S. Fukuzumi, J. Am. Chem. Soc. 122 (2000) 5733.
[32] S. Fukuzumi, H. Imahori, H. Yamada, M.E. El-Khouly, M. Fujitsuka, O. Ito, D.M. Guldi, J. Am. Chem. Soc. 123 (2001) 2571.
[33] S. Fukuzumi, K. Ohkubo, Chem. Eur. J. 6 (2000) 4532.
[34] S. Fukuzumi, M. Patz, T. Suenobu, Y. Kuwahara, S. Itoh, J. Am. Chem. Soc. 121 (1999) 1605.
[35] S. Fukuzumi, T. Suenobu, M. Patz, T. Hirasaka, S. Itoh, M. Fujitsuka, O. Ito, J. Am. Chem. Soc. 120 (1998) 8060.
[36] M. Patz, Y. Kuwahara, T. Suenobu, S. Fukuzumi, Chem. Lett. (1997) 567.
[37] R.N. Bagchi, A.M. Bond, F. Scholz, R. Stösser, J. Am. Chem. Soc. 111 (1989) 8270.
[38] K. Dyrek, M. Che, Chem. Rev. 97 (1997) 305.
[39] M. Che, A.J. Tench, Adv. Catal. 32 (1983) 1.
[40] E. Giamello, Z. Sojka, M. Che, A. Zecchina, J. Phys. Chem. 90 (1986) 6084.
[41] Z. Sojka, E. Giamello, M. Che, A. Zecchina, K. Dyrek, J. Phys. Chem. 92 (1988) 1541.
[42] (a) W. Känzig, M.H. Cohen, Phys. Rev. Lett. 3 (1959) 509; (b) H.R. Zeller, W. Kanzig, Helv. Phys. Acta 40 (1967) 845.
[43] P.H. Kasai, J. Chem. Phys. 43 (1965) 3322.
[44] (a) J.H. Lunsford, Catal. Rev. 8 (1973) 135; (b) M. Che, Chem. Rev. 97 (1997) 305.
[45] S. Fukuzumi, T. Okamoto, J. Am. Chem. Soc. 115 (1993) 11600.
[46] S. Fukuzumi, S. Mochizuki, T. Tanaka, Inorg. Chem. 28 (1989) 2459.
[47] D.T. Saywer, T.S. Calderwood, K. Yamaguchi, C.T. Angelis, Inorg. Chem. 22 (1983) 2577.
[48] S. Fukuzumi, Bull. Chem. Soc. Jpn. 70 (1997) 1.
[49] S. Fukuzumi, in: V. Balzani (Ed.), Electron Transfer in Chemistry, vol. 4, Wiley–VCH, Weinheim, 2001, pp. 3–57.
[50] I. Fridovich, Annu. Rev. Biochem. 64 (1995) 97.
[51] A. Bencini, I. Bertini, D. Gatteschi, A. Scozzafava, Inorg. Chem. 17 (1978) 3194.
[52] P.J. Hart, M.M. Balbirnie, N.L. Ogihara, A.M. Nersissian, M.S. Weiss, J.S. Valentine, D.A. Eisenberg, Biochemistry 38 (1999) 2167.
[53] H. Ohtsu, S. Fukuzumi, Chem. Eur. J. 7 (2001) in press.
[54] H. Ohtsu, S. Fukuzumi, Angew. Chem. Int. Ed. Engl. 39 (2000) 4537.
[55] N. Kitajima, K. Fujisawa, Y. Moro-oka, K. Toriumi, J. Am. Chem. Soc. 111 (1989) 8975.
[56] K.A. Magnus, B. Hazes, H. Ton-That, C. Bonaventura, J. Bonaventura, W.G.J. Hol, Proteins: Struct. Funct. Genet. 19 (1994) 302.
[57] K.A. Magnus, H. Ton-hat, J.E. Carpenter, Chem. Rev. 94 (1994) 727.
[58] S. Itoh, T. Kondo, M. Komatsu, Y. Ohshiro, C. Li, N. Kanehisa, Y. Kai, S. Fukuzumi, J. Am. Chem. Soc. 117 (1995) 4714.
[59] S. Itoh, H. Nakao, L.M. Berreau, T. Kondo, M. Komatsu, S. Fukuzumi, J. Am. Chem. Soc. 120 (1998) 2890.
[60] K. Fujisawa, M. Tanaka, Y. Moro-oka, N. Kitajima, J. Am. Chem. Soc. 116 (1994) 12079.
[61] J.A. Halfen, S. Mahapatra, E.C. Wilkinson, S. Karderli, V.G. Young Jr., L. Que Jr., A.D. Zuberbühler, W.B. Tolman, Science 271 (1996) 1397.
[62] C.J. Cramer, B.A. Smith, W.B. Tolman, J. Am. Chem. Soc. 118 (1996) 11283.
[63] H. Imahori, K. Tamaki, D.M. Guldi, C. Luo, M. Fujitsuka, O. Ito, Y. Sakata, S. Fukuzumi, J. Am. Chem. Soc. 123 (2001) 2607.

[64] S. Fukuzumi, H. Imahori, in: V. Balzani (Ed.), Electron Transfer in Chemistry, vol. 2, Wiley–VCH, Weinheim, 2001, pp. 927–975.
[65] S. Fukuzumi, D.M. Guldi, in: V. Balzani (Ed.), Electron Transfer in Chemistry, vol. 2, Wiley–VCH, Weinheim, 2001, pp. 270–327.
[66] M. Fujitsuka, O. Ito, H. Imahori, K. Yamada, H. Yamada, Y. Sakata, Chem. Lett. (1999) 721.
[67] K. Yamada, H. Imahori, Y. Nishimura, I. Yamazaki, Y. Sakata, Chem. Lett. (1999) 895.
[68] C. Luo, D.M. Guldi, H. Imahori, K. Tamaki, Y. Sakata, J. Am. Chem. Soc. 122 (2000) 6535.